



OPTIMUM DESIGN OF ARAMID-PHENOLIC/GLASS-PHENOLIC COMPOSITE JOURNAL BEARINGS

Ha Na Yu*, Seong Su Kim*, Seong Nam Kim**, Suzuki Kazuwoshi**, Dai Gil Lee*

*Department of Mechanical Engineering, Korea Advanced Institute of Science and Technology, ME3221, Guseong-dong, Yuseong-gu, Daejeon 305-701, Republic of Korea,

**Sam Sung Heavy Industries, Janpying-ri, Shinhyen-eup, Goeje City, South Gyeongsang Province, 656-710, Republic of Korea

Keywords: *Composite journal bearing, Aramid-phenolic/glass-phenolic, CTE, Interference fitting*

Abstract

White or babbit bearing materials for the journal bearing liner have seizure problem during the start and stop periods of journals or when the applied pressure on the bearing is severe, while composite materials can eliminate the seizure problem between the journal and the bearing. So, the composite journal bearings are increasingly employed in large journal bearings for marine application.

Asbestos-phenolic had been used for the materials of the composite bearings because of the outstanding performance per price, although the health hazard of this material is recently a great concern.

Recently aramid/glass reinforced phenolic composite journal bearings have been employed rather than the asbestos-phenolic composite bearings for the large marine bearing. However, the failures of aramid/glass reinforced phenolic composite journal bearings have occurred.

In this work, the mechanical properties of aramid/glass reinforced phenolic composite were measured for the stress analysis of the journal bearing with finite element method. The failure modes of the aramid/glass reinforced phenolic composite journal bearings were observed from the failed bearings. The modified dimensions of aramid/glass reinforced phenolic composite journal bearings and optimum interference fit amount were suggested using the FE-analysis results.

1 Introduction

White or babbit bearing materials for the liners of large marine bearings have seizure problem during the start and stop periods of journals or when the applied pressure on the bearing is severe, while composite journal bearings can eliminate the seizure problem between journals and bearings [1]. Therefore, the phenolic composite bearings are employed in journal bearings for marine application and mainly asbestos-phenolic have been used for the materials of the composite marine bearings due to its high performance per price although the health hazard of asbestos fiber has been great concern.

Phenolics among several types of plastics for bearings are mainly used because the phenolics operate satisfactory with steel or bronze journals when lubricated with oil, water, or other liquids [2]. They have good resistance to seizure. But one main disadvantage of the phenolics is its low thermal conductivity (0.35 W/m·K), which is about 1/150 of steel. The low thermal conductivity of phenolics hinders the dissipation of heat generated in bearing, which can result in bearing failure by charring.

Asbestos-phenolic journal bearings, which had been used for so long, are vulnerable to failure due to the stress concentration in grooves for the passage of lubricant oil, the thermal stresses caused by the difference of coefficient of thermal expansion (CTE) between the composite bearing and the steel housing, and the interference fitting during assembly of the composite bearing in steel housing [3].

Journal bearings made of aramid-phenolic/glass-phenolic composite, a hybrid composite, have been employed for the large composite journal bearings, however, the materials still have the same problems of other composite bearing materials. Although the desired operating condition of journal bearings is full film lubrication,

mixed and boundary lubrications are inevitable during the start and stop periods, or under severe working conditions, such as insufficient lubricant supply and heavy loading, which increases the operating temperatures of the bearing and lubrication oil. In this situation, the dimensional change of phenolic composites is inevitable because of their low thermal conductivity and the difference of CTEs of two materials [4].

In this work, the mechanical properties of the aramid-phenolic/glass-phenolic composite were measured for the stress analysis of the composite journal bearings using finite element method. The causes of the failure of the aramid-phenolic/glass-phenolic composite journal bearings were investigated. Finally, the modified dimensions of the aramid-phenolic/glass-phenolic composite journal bearings and the optimal interference fit amount were suggested using the results of finite element method [5].

2 Bearing configurations

The shape of the composite journal bearing whose outer diameter is about 1.0 m is shown in Fig. 1. Fig. 2 shows the top and bottom inner surfaces of the composite bearing which were charred due to overheat. The several scored marks were more pronounced on the bottom surface. The composite bearing was composed of the aramid-phenolic and glass-phenolic composites, as shown in Fig.1. All the cracks were initiated and propagated through the interface between the aramid and glass-phenolic composite in the fiber direction as shown Fig. 2.

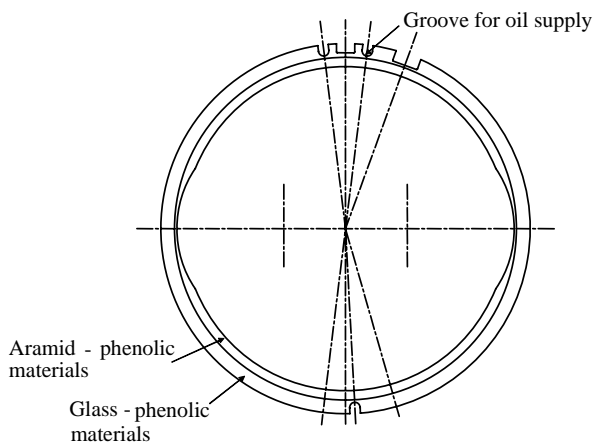


Fig. 1. Shape of composite journal bearing

3 Properties of the aramid/glass reinforced phenolic composite

3.1 Material preparation

The aramid and the glass fiber were composed of several bundles of strands. The aramid fibers impregnated with phenolic resin was wound first, then followed the glass fibers impregnated with phenolic resin. The composite material had large void volume fraction due to the winding operation. The fiber volume fraction of the glass-phenolic composite was measured with the ignition loss method [6], while the fiber volume fraction of the aramid-phenolic composite was obtained by measuring the fiber area of the cross section of the photograph by SEM (Scanning electronic microscope) [7]. Table 1 shows the average fiber, resin and void volume fractions of aramid/glass-phenolic composite.

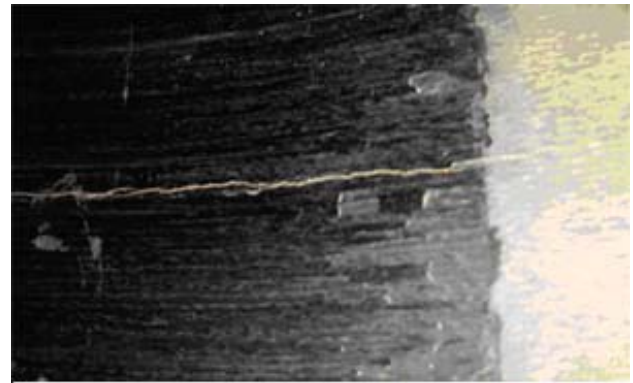


Fig. 2. Radial cracks and surface exfoliation on the inner surface of a composite journal bearing

Table 1. Volume fractions of fiber and matrix

	ν_f	ν_m (Phenol)	ν_v (Void)
Glass-phenolic	0.33	0.55	0.12
Aramid-phenolic	0.47	0.41	0.12

3.2 TMA test

The CTEs of composite materials were obtained by measuring the dimensional change of aramid/glass-phenolic specimens with respect to temperature change from 40°C to 190°C. The CTEs in the three principal material coordinate systems are denoted by α_1 , α_2 , and α_3 as shown in Fig. 3. Since the filament winding angle during the fabrication was chose to 90°, the hoop direction was the fiber direction.

The heating rate for each specimen was 5°C/min and the dimensional changes were recorded

with a TMA Analyzer (TA Instrument, USA). The test results were plotted in Figs. 4, 5 and the CTEs listed in Table 2 were estimated by the mean slopes of curves, whose range was from 50°C to 160°C. The aramid-phenolic composite had the CTE in fiber direction less than zero due to negative CTE of the aramid fiber [4], while the glass-phenolic composite had positive CTEs in all the directions.

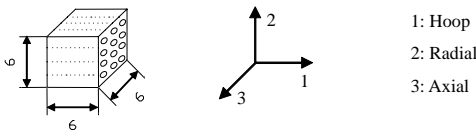


Fig. 3. Shape of specimen for TMA

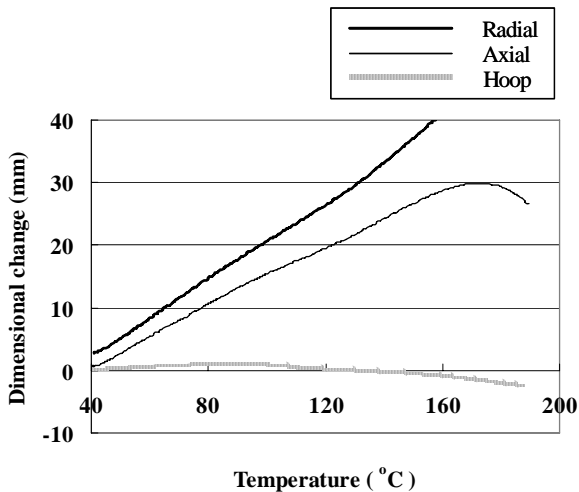


Fig. 4. TMA test results of aramid-phenolic composites

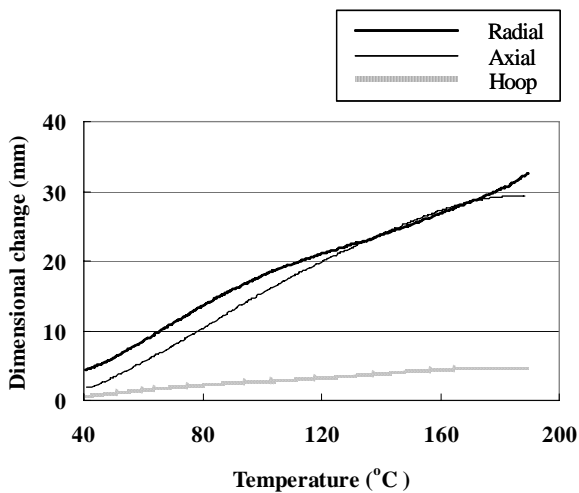


Fig. 5. TMA test results of glass-phenolic composites

Table 2. Coefficients of thermal expansion (CTE) of composite bearing material [$\mu/\text{°C}$]

	Radial	Axial	Hoop	
Aramid-phenolic	54.54	39.81	50°C ~ 80°C	3.083
			100°C ~ 160°C	-4.764
Glass-phenolic	31.98	36.87	5.164	

(Linearization from 50°C to 160°C)

3.3 Swelling test

The model developed to describe the penetration of oil into aramid/glass-phenolic material is based on the anisotropic nature of the composite material [3].

In this test, the specimens for swelling were prepared from the real bearing. The size of specimens was determined according to ASTM D 5515-97 [8] as shown in Fig. 6. These specimens were immersed in SAE 30 oil for 10 days under the oil temperatures of 30°C. The swelling rate is defined as follows.

$$\text{Swelling rate (\%)} = \frac{L_a - L_b}{L_b} \times 100 \quad (1)$$

where L_a = Length after immersion
 L_b = Length before immersion

The swelling data measured at 30°C are listed in Table 3.

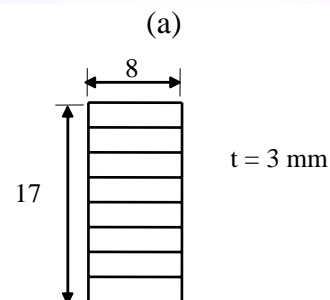
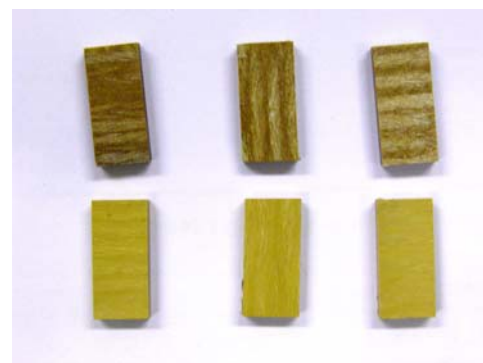


Fig. 6. Specimens for swelling test: (a) Photograph, (b) Dimension

Table 3. Swelling of aramid/glass-phenolic material at 30°C

	ε_z (%)	ε_θ (%)	ε_r (%)
Aramid-phenolic	0.014	0.040	0.047
Glass-phenolic	0.0091	0.070	-0.042

3.4 Mechanical properties

Since the compressive strength [9] is most important for the journal bearing, they were measured at room temperature (25°C), 30°C and 80°C with and without SAE 30 oil. Table 4 shows the compressive strength with respect to temperature. As shown in Fig. 7, the compressive strength decreased as the temperature was increased. Especially, the reduction of the compressive strength with respect to temperature in the hoop direction was larger than other two directions.

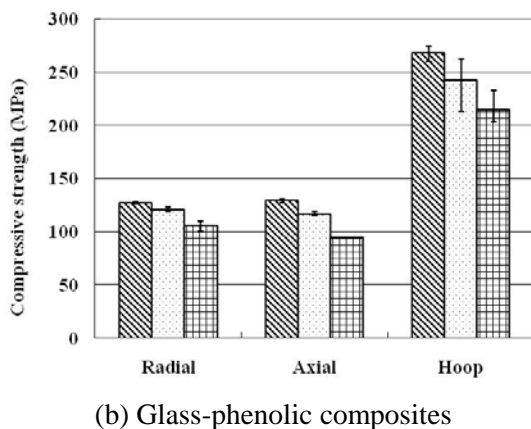
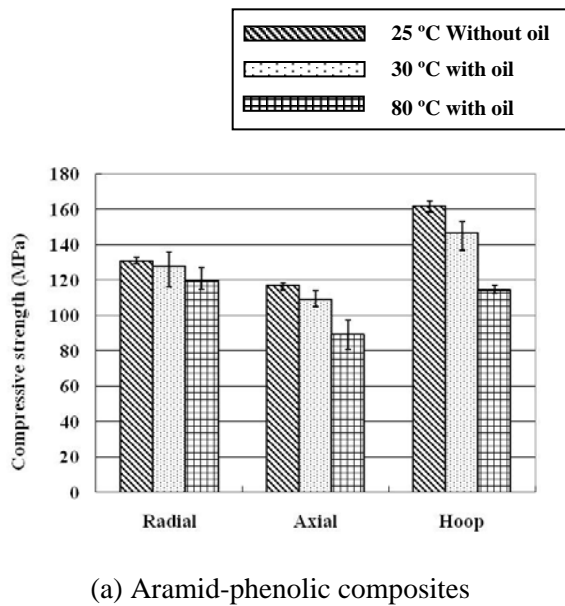


Fig. 7. Compressive strength w.r.t. temperature

Table 4. Compressive strength aramid/glass-phenolic composites [MPa]

	temperature	1(hoop)	2(radial)	3(axial)
Aramid-phenolic	25°C	162	130	117
Glass-phenolic		268	127	129
Aramid-phenolic	30°C	146	128	109
Glass-phenolic		242	121	116
Aramid-phenolic	80°C	114	119	89.0
Glass-phenolic		215	105	94.3

Table 5. Tensile strength and elastic modulus of aramid/glass-phenolic composite material

	Materials	1(hoop)	2(radial)	3(axial)
Tensile strength [MPa]	Aramid-phenolic	94.1	11.6	11.6
	Glass-phenolic	98.9	8.48	8.48
Elastic modulus [GPa]	Aramid-phenolic	9.50	2.57	2.57
	Glass-phenolic	23.2	4.53	4.53

Table 6. Poisson's ratio of aramid/glass-phenolic composite material

	ν_{12}	ν_{13}	ν_{23}
Aramid-phenolic	0.428	0.428	0.543
Glass-phenolic	0.389	0.389	0.887

The tensile test specimens were prepared according to ASTM D 3039M-95a [10]. Tables 5 and 6 show the test results.

The shape of specimen for shear test is shown in Fig. 8 [3]. The '1' direction means the fiber (hoop) direction of the journal bearing. The '2' and '3' directions mean the radial and axial directions, respectively. Two biaxial strain gauges were attached to the both sides of specimen with $\pm 45^\circ$ angle. For the specimen in the 1-3 plane, the delamination between laminas occurred, while for the specimen in the 2-3 plane, the failure occurred after the crack initiated.

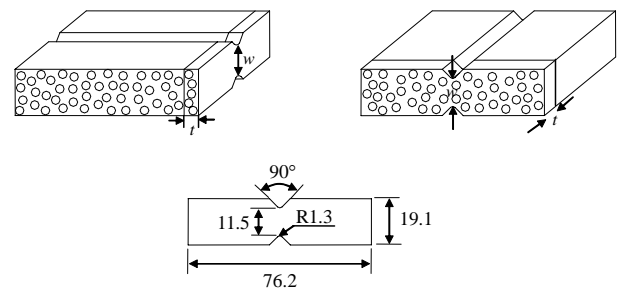


Fig. 8. Shape of specimen for Iosipescu test (1–3, 2–3 directions)

The mean shear stress was obtained by dividing load with cross-sectional area at the notch as follows.

$$\tau_{avg} = \frac{P}{wt} \quad (2)$$

where w = distance between the notches
 t = thickness of the specimen

The shear strain γ_{gage} is

$$\gamma_{gage} = \varepsilon_{-45^\circ} - \varepsilon_{+45^\circ} \quad (3)$$

where ε_{-45° : tensile strain

ε_{+45° : compressive strain

The shear modulus G was calculated from the shear stress - strain graph as follows.

$$G = \frac{\tau_{avg}}{\gamma_{gage}} \quad (4)$$

In this work, based on the ASTM D5379 [11], the chord modulus was obtained from 0.1% to 0.6% of strain because the failure strains in both planes (1-3, 2-3) were larger than 1.8%. Table 7 shows the test results, in which the shear strength and shear stiffness in the 1-3 plane were three and two times larger than those in the 2-3 plane.

Table 7. Shear test results

	Materials	1-3 direction	2-3 direction
Shear strength [MPa]	Aramid-phenolic	43.8	11.5
	Glass-phenolic	48.3	9.63
Shear modulus [GPa]	Aramid-phenolic	1.20	0.833
	Glass-phenolic	2.17	1.20

3.5 Wear test

During the start and stop periods, the journal and the bearing may directly contact each other. To investigate the contact problem, the friction coefficient and the wear volume of the aramid-phenolic composite were measured due to the damage occurred on the inner surface of the bearing. Since the interference fitting between the bearing and the steel housing was used to assemble the bearing, the friction coefficient and wear volume of the glass-phenolic composite were also measured.

In this test, the specimens were cut to the size of 5 mm × 5 mm × 6 mm. The wear tests were performed using a pin-on-disk type arrangement [12]. The steel disk was 240 mm in diameter and 12

mm in thickness. During the wear test of composite specimens, the PV value (P : pressure, V : speed) of 0.4 MPa·m/s was used, which was similar to the actual operating condition of large journal bearing for oil tankers. The friction coefficient and wear volume were listed in Table 8.

Table 8 Friction coefficients and wear volume of aramid/glass-phenolic composites

	Aramid-phenolic		Glass-phenolic	
	Parallel	Perpendicular	Parallel	Perpendicular
Wear volume (mm ³)	1.29	0.757	5.30	10.3
Friction coefficient	0.383	0.396	0.663	0.716

4 Finite element analysis of the composite journal bearing

4.1 Modeling

Using the material properties obtained, the stress and strain distributions were calculated by modeling the composite journal bearing under the assumed operating conditions using finite element method. The major assumption was that the temperature and pressure of the composite bearing were equal to the mean values of the lubrication oil. In case of real journal bearings, the temperature and pressure continuously change, therefore, they are locally different. In this work, however, the nominal bearing pressure and mean temperature rise were used to investigate the macroscopic deformation of composite bearing. The mean temperature rise was calculated by adding two contributions such as the actual mean temperature rise of the oil film and the equivalent temperature rise to give the same dimensional change due to bearing swelling caused by oil penetration.

$$\Delta T_{total} = \Delta T_{film} + \Delta T_{swelling} \quad (5)$$

where ΔT_{film} = Temperature rise of oil film,

$\Delta T_{swelling}$ = Equivalent temperature rise by swelling

The equivalent temperature rise of 8°C due to swelling was obtained by dividing the swelling strain with the CTE of the composite. The mean temperature rise of oil film was 25°C under the average pressure of 0.68 MPa. Therefore, the estimated total mean temperature rise was 33°C.

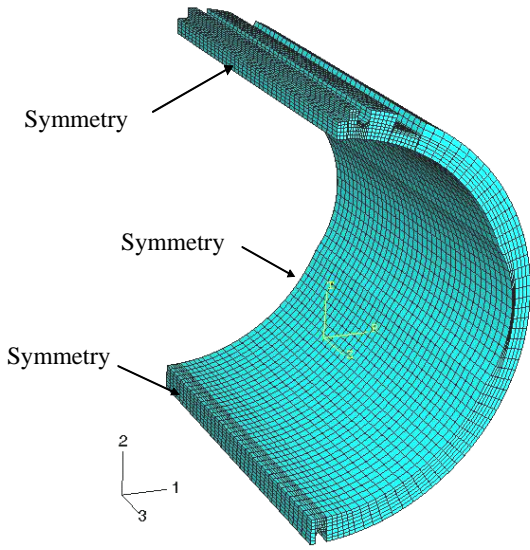


Fig. 9. Modeling of the aramid/glass-phenolic bearing for FE-analysis

The journal bearing was assembled to the steel housing with the radial interference fit amount of 450 μm [3]. Since most heat generated in the oil film flew out through the side leakage of oil due to the higher heat capacity of oil than that of steel, the steel housing was assumed as a rigid body. The friction coefficient between the steel housing and the composite bearing was 0.66. Only one fourth of the composite bearing was analyzed for computational efficiency as shown in Fig. 9. The symmetry boundary conditions were used for the cross-sectional area as shown in Fig. 9 and all the translational and rotational nodes of the housing were fixed. The conditions of interference fit of the composite bearing were adjusted by the temperature change. The nominal bearing pressure of 0.68 MPa was given on the inner surface of the composite bearing and the temperature of bearing was increased to 33°C.

4.2 Stress analysis results

The FE-analysis results show that the maximum compressive stress is 168.5 MPa in the hoop direction at the center of groove which is used for passage of oil supplying pipe as shown in Fig. 10. Since this value is higher than the compressive strength 162 MPa of the aramid-phenolic composite, and lower than that of the glass-phenolic composite, 268 MPa, the failure of composite bearing might occur along the grooves even the journal bearing operates in stable condition. The FE-analysis results

show that the maximum shear stress at the interface is 12.7 MPa, which is higher than the shear strength of aramid-phenolic and glass-phenolic in the 2-3 plane as shown in Fig. 11. The crack might occur at this interface and propagate to the inner surface of aramid-phenolic composite. This location of failure coincides with one of the failed real composite journal bearing in Fig. 2.

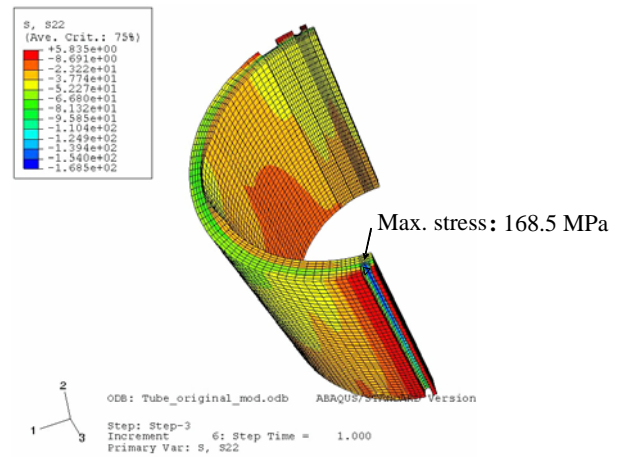


Fig. 10. Compressive stress distribution in the hoop direction

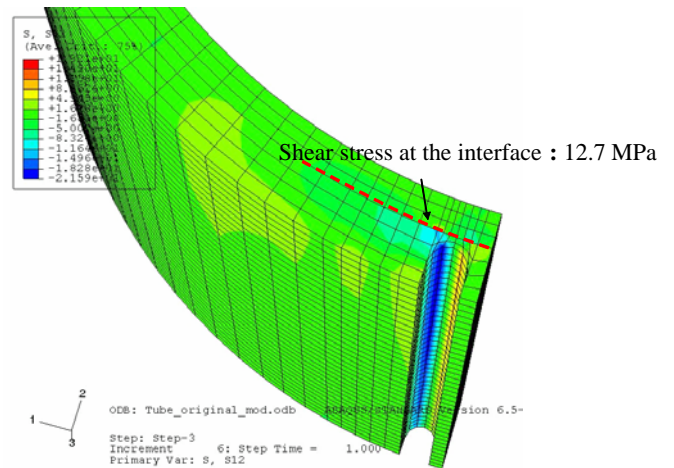


Fig. 11. Shear stress distribution in 2-3 plane

Since the aramid-phenolic liner has low thermal conductivity, the temperature of bearing was assumed to increase to 80°C, which was used in the finite element model. The compressive stress in the hoop direction increased to 201 MPa and the shear stress at the interface also increased to 15 MPa. Therefore, the failure index at 80°C might be higher than at 33°C. The maximum compressive stress in

the hoop direction and the shear stress at the interface with respect to temperature were listed in Table 9.

4.3 Optimal design

The failure in the aramid/glass-phenolic composite journal bearing occurred due to the compressive stress in the hoop direction and the shear stress at the interface. To reduce the failure of the composite bearing, the design of composite bearing was optimized as follows. First, the experiment points about the geometry of the journal bearing were determined using the DOE (Design of experiments) method [13] and the finite element models were constructed respectively. Second, the compressive stress, which was an objective function, was expressed as a function of the ratio of the two kinds of the materials and the interference fit amount. Finally, the optimal parameters to minimize the compressive stress of the journal bearing were obtained by using the response surface method [13].

4.3.1 Algorithm for the optimal design

Design of experiments is an efficient method when the experiment variables are too many or the experiment could not be performed case by case. The response surface method usually is used to improve the structural design when the basic design was given. In the response surface method, the objective function and the constraints should be represented as the function of the variables. In this work, minimization of the compressive stress in the hoop direction was the objective function, and the constraint condition was no slip between the bearing and the steel housing. The design parameters were the volume ratio of two kinds of materials and the interference fit amount. If the objective function and the constraints were expressed as the second order function of two variables, they could be written as follows [13].

$$f(r,t) = a_0 + a_1r + a_2t + a_3r^2 + a_4t^2 + a_5rt \quad (6)$$

$$g(r,t) = b_0 + b_1r + b_2t + b_3r^2 + b_4t^2 + b_5rt \geq \text{Min. friction force (for the non slip condition)} \quad (7)$$

Where

$f(r,t)$ = maximum compressive stress in the journal bearing

$g(r,t)$ = friction force between the bearing and the steel housing

r = ratio of volume content of aramid-phenolic composite over total volume

t = interference fit amount between the bearing and the steel housing

The maximum compressive stress and the frictional force were known from the finite element analysis and the coefficients of these functions were calculated using the least square method. The objective function and the constraints were obtained as follows.

$$f(r,t) = -1009 + 2399r + 1201t - 1724r^2 - 1151a_4t^2 + 102rt \quad (MPa)$$

$$g(r,t) = -22.34 + 59.68r + 26.75t - 45.47r^2 - 23.27t^2 - 1.758rt \quad (kN)$$

$$0.450 \leq r \leq 0.1$$

$$0 \leq t \leq 1.0 \text{ (mm)} \quad (8)$$

To find the optimal point of these functions, the Lagrangian multiplier was applied and the optimal design parameters were calculated using the numerical method [14].

$$\text{Optimal design parameter } (r,t) = (0.459, 0.352) \quad (9)$$

As shown Fig. 12, the optimal point of the minimum compressive stress in the objective function surface above the constraints surface was selected for no slip condition between the bearing and steel housing.

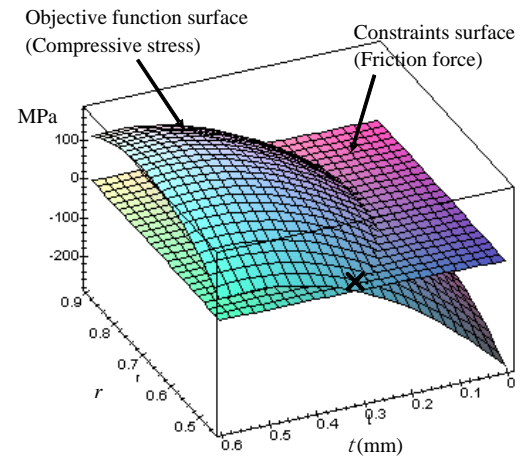


Fig. 12. Surfaces of the objective function and the constraints

4.3.2 Stress analysis results in the optimal design

All experimental FE-analysis results showed that the maximum compressive stress in the hoop

direction occurred at the center of grooves in top and bottom of the bearing. The maximum compressive stress of 67.3 MPa from the optimal design parameters occurred at the same place. The maximum compressive stress decreased about 60 % compared to the compressive stress of 168 MPa in the previous design. Also, the shear stress at the interface decreased from 12.7 MPa to 3.17 MPa. The friction force of 2.52 kN obtained from the FE-analysis was higher than the minimum friction force of 1.59 kN to prevent the slip between the bearing and steel housing. The maximum compressive stress in the hoop direction and the shear stress at the interface in optimal design were listed in Table 8. The results of optimization process show that the values of optimal design parameters were lower than that of the conventional design parameters. As the volume content of the aramid-phenolic composite decreases, the bearing stiffness increases because the stiffness of the glass-phenolic composite is higher than that of the aramid-phenolic composite. Also, a thin aramid-phenolic composite might be used as a liner material because it has the lower friction coefficient and higher compatibility than that of the glass-phenolic composite.

Table 9. Max. compressive stress and shear stress w.r.t. temperature and design parameters [MPa]

	ΔT	Max. compressive stress in the hoop direction	Shear stress at the interface
Conventional design	33°C	168	12.7
	80°C	201	15.0
Optimal design	33°C	67.3	3.17
	80°C	72.8	3.54

5 Conclusions

In this work, the failure of large aramid/glass reinforced phenolic composite journal bearing for marine application was investigated by FEM stress analysis. The stress analysis results show that the maximum compressive stress in the hoop direction occurred at the groove for oil passage due to the interference fit amount. The different coefficient of thermal expansion between the aramid and glass-phenolic composites induced high shear stress at the interface, which caused the crack to propagate into the inner surface of the bearing. The other causes of the failure were the large interference fit amount between the bearing and housing and the improper

volume ratio of the two kinds of materials. By adjusting the ratio of two kinds of bearing materials and giving the optimal interference amount, the design reduced the maximum compressive stress 60% and the shear stress at the interface 70 % at 33°C.

6 Acknowledgment

This work was supported by the NRL phase II project and in part BK21 of Korean Government. The authors wish to acknowledge the cooperation of Samsung Heavy Industries Ltd. (Korea) in executing this project.

7 References

- [1] Suh N.P. "Tribophysics". Prentice-Hall, Inc., 1986.
- [2] Bernard J. Hamrock "Fundamentals of Fluid Film Lubrication". McGraw-Hill, Inc., 1994.
- [3] Lee D.G., Kim S.S. "Failure analysis of asbestos-phenolic composite journal bearing". Composite structures, Vol. 65, 37-46, 2004.
- [4] Lee D.G., Suh N.P. "Axiomatic design and fabrication of composite structures". Oxford, 2006.
- [5] Shigley JE, Mischke CR "Mechanical engineering design". 7-edition, McGraw-Hill, 1989.
- [6] ASTM Standard (D2584-02) "Standard test method for ignition loss of cured reinforced resin". ASTM 100 Barr Harbor Drive, West Conshohocken, PA 19428, 1997.
- [7] Ronald F. Gibson "Principles of composite material mechanics". McGraw-Hill, Inc., 1994.
- [8] ASTM Standard (D 5515-97) "Standard test methods for determination of the swelling properties of bituminous coal using a dilatometer". ASTM 100 Barr Harbor Drive, West Conshohocken, PA 19428, 1997.
- [9] British Standard BS2728 (Method 345A) "Method of testing plastics : Determination of compressive properties". British Standard Institute, UK, 1992.
- [10] ASTM Standard (D 3039/D 3039M-95a) "Standard test methods for tensile properties of polymer matrix composite materials". ASTM 100 Barr Harbor Drive, West Conshohocken, PA 19428, 1997.
- [11] ASTM Standard (D 5379/D 5379M-93) "Standard test methods for shear properties of composite materials by the v-notched beam method". ASTM 100 Barr Harbor Drive, West Conshohocken, PA 19428, 1997.
- [12] Kim S.S., Lee H.G., Lee D.G. "Tribological behaviors of carbon composite grooved surfaces". Composite structures, Vol. 71, 238-245, 2005.
- [13] Cox D. R. "The theory of the design of experiments". Chapman & Hall/CRC, 2000.

[14] Jasbir S. Arora "Introduction to optimum design".
McGraw-Hill, Inc., 1994.